

This article was downloaded by: [Tomsk State University of Control Systems and Radio]

On: 17 February 2013, At: 06:00

Publisher: Taylor & Francis

Informa Ltd Registered in England and Wales Registered Number: 1072954

Registered office: Mortimer House, 37-41 Mortimer Street, London W1T 3JH, UK



## Molecular Crystals

Publication details, including instructions for authors and subscription information:

<http://www.tandfonline.com/loi/gmcl15>

## $\gamma$ -Radiation Induced Color Centers in Anthracene

Haywood Blum<sup>a</sup>, P. L. Mattern<sup>a</sup>, R. A. Arndt<sup>a</sup> & A. C. Damask<sup>b c</sup>

<sup>a</sup> Brookhaven National Laboratory, Upton, N.Y.

<sup>b</sup> Brookhaven National Laboratory, Upton, N.Y.

<sup>c</sup> Queens College, The City University of N.Y., Flushing, N.Y.

Version of record first published: 21 Mar 2007.

To cite this article: Haywood Blum, P. L. Mattern, R. A. Arndt & A. C. Damask (1967):  $\gamma$ -Radiation Induced Color Centers in Anthracene, *Molecular Crystals*, 3:2, 269-280

To link to this article: <http://dx.doi.org/10.1080/15421406708083443>

PLEASE SCROLL DOWN FOR ARTICLE

Full terms and conditions of use: <http://www.tandfonline.com/page/terms-and-conditions>

This article may be used for research, teaching, and private study purposes. Any substantial or systematic reproduction, redistribution, reselling, loan, sub-licensing, systematic supply, or distribution in any form to anyone is expressly forbidden.

The publisher does not give any warranty express or implied or make any representation that the contents will be complete or accurate or up to date. The accuracy of any instructions, formulae, and drug doses should be independently verified with primary sources. The publisher shall not be liable for any loss, actions, claims, proceedings, demand, or costs or damages

whatsoever or howsoever caused arising directly or indirectly in connection with or arising out of the use of this material.

## $\gamma$ -Radiation Induced Color Centers in Anthracene<sup>†</sup>

HAYWOOD BLUM, P. L. MATTERN, and R. A. ARNDT

Brookhaven National Laboratory, Upton, N.Y.

and

A. C. DAMASK

Brookhaven National Laboratory, Upton, N.Y. and Queens College,  
The City University of N.Y., Flushing, N.Y.

*Received June 13, 1967*

**Abstract**—The effects of  $\gamma$ -irradiation on pure anthracene have been investigated by optical absorption and electron paramagnetic resonance (EPR) measurements. It is found that the optical absorption peaks which are produced by the radiation at 30°C are stable at 30°C but increase upon annealing up to 140°C; the most prominent of these being at 6060 Å and 5350 Å. EPR signals arising from irradiation are stable to 140°C but do not grow between 30°C and 140°C. Both optical density and EPR signals decrease upon annealing above 190°C. A model is proposed to explain the nature of the EPR signals based upon cross-linking of the anthracene molecules.

### Introduction

It is well known that high energy irradiation of organic molecules can both ionize them and break bonds. Radicals formed in this way can give rise to EPR signals and optical absorption. Adjacent radicals in condensed systems are able to cross-link. The present investigation of  $\gamma$ -irradiated anthracene was begun as an initial study of the above phenomena in highly pure single crystals of the aromatic hydrocarbons.

<sup>†</sup> Work supported by the U.S. Atomic Energy commission and the U.S. Army Research Office, Durham.

### Material Preparation and Experimental Procedure

The anthracene used in this work came from two sources. The Harshaw Chemical Company supplied optical quality, single crystals of scintillator grade anthracene. Most of the EPR measurements were made using these Harshaw crystals. The second source was K&K Chemicals who supplied technical grade ( $\sim 98\%$  pure) anthracene powder. This powder was purified by chromatographic separation, vacuum sublimation, and zone refining.<sup>1</sup> Single crystals about 1 cm in diameter were grown from a melt of this purified material in a Bridgman-type furnace. Plates about 2 mm thick were cleaved from these crystals for the optical density measurements; anthracene cleaves parallel to the *ab* plane. Optical absorption and electrical measurements (e.g. drift mobility measurements such as those performed by Hoesterey and Letson<sup>2</sup>) indicated that the impurity concentration of these plates was of the order of a few parts per million.

Samples were irradiated in a  $\text{Co}^{60}$  gamma-pool at approximately  $30^\circ\text{C}$ ; some, irradiated at a higher temperature, were packed in anthracene powder to reduce surface sublimation. As a control, to see if any of the effects were due to diffusion into the crystal of surface products, two additional samples were irradiated in vacuo, one at ambient temperature and the other at  $120^\circ\text{C}$ .

The EPR measurements were made in a conventional manner using an X-band spectrometer. Optical density measurements were made with a Cary 14 spectrophotometer having only air in the reference beam compartment. In order to obtain a baseline for the radiation induced peaks, each run on the spectrophotometer was started sufficiently in the infra-red region to allow corrections to be made for scattering from the crystals.

Annealing of the crystals was carried out isochronally using steps of  $10^\circ\text{C}$ , starting at  $40^\circ\text{C}$ , and 45 minute intervals. The crystals were annealed in air but packed in anthracene powder to reduce surface sublimation; the crystals irradiated in vacuo at ambient temperature were also annealed in vacuo. Crystals were not annealed above  $200^\circ\text{C}$  because, even though they were packed

in anthracene powder, too much light scattering resulted from surface roughening due to sublimation. Unless stated otherwise, all measurements were made at room temperature.

## Results

After  $\text{Co}^{60}$   $\gamma$ -irradiation of  $10^7$  to  $10^8$  r, anthracene turns a dark, brown-yellow color. Optical measurements show a broad back-

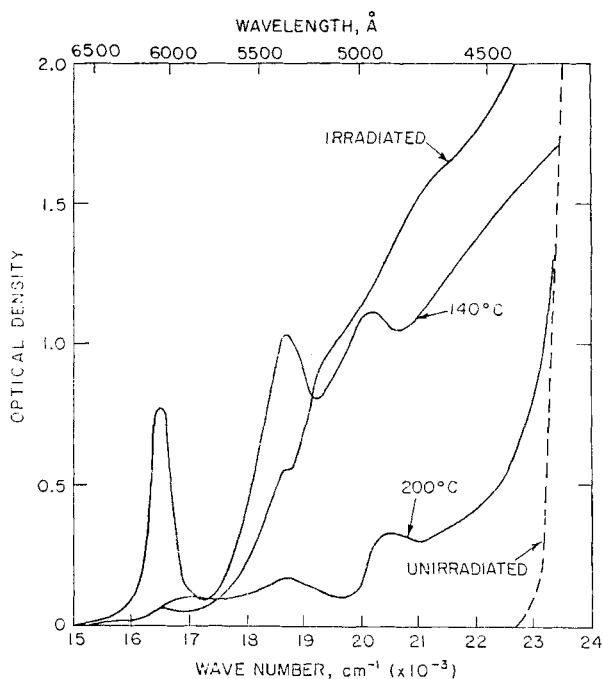


Figure 1. Optical density of anthracene crystals as a function of wave length. The 140°C and 200°C indicate annealing temperature following  $\gamma$ -irradiation.

ground absorption, overlapping the band edge of anthracene, with small peaks at 6320 Å, 6060 Å and 5350 Å ( $15.8 \times 10^3 \text{ cm}^{-1}$ ,  $16.5 \times 10^3 \text{ cm}^{-1}$  and  $18.7 \times 10^3 \text{ cm}^{-1}$ , respectively). Figure 1 shows a typical spectrum taken at room temperature for a crystal receiving  $1.48 \times 10^8$  r at a dose rate  $8.36 \times 10^6$  r/hr. Within experimental

error, the optical absorption is independent of dose rate for rates from  $5.60 \times 10^5$  r/hr to  $8.36 \times 10^6$  r/hr and linearly dependent on dose from  $1.23 \times 10^7$  r to  $1.48 \times 10^8$  r.

An EPR signal, such as that shown in Fig. 2 can be seen for doses greater than  $\sim 5 \times 10^6$  r. This signal grows in strength approximately linearly with dose up to  $10^9$  r, the heaviest irradiation dose

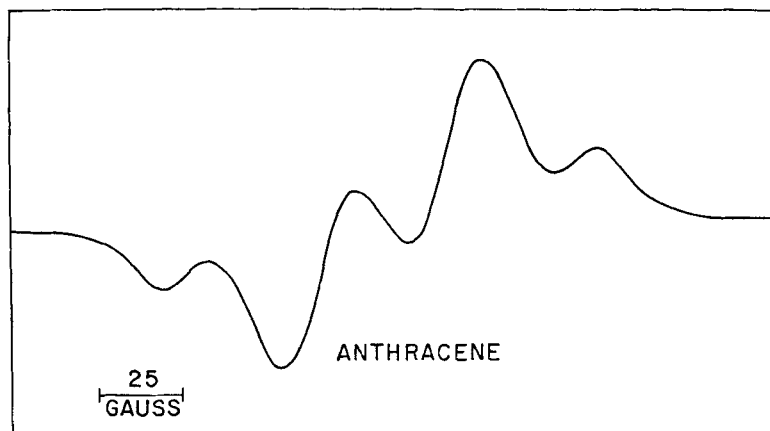


Figure 2. Typical EPR absorption derivative as a function of external magnetic field of  $\gamma$ -irradiated anthracene.

used. No saturation in the growth rate of the signal with dose was found. The spectrum of Fig. 2 can be described accurately as four equally spaced Gaussian lines with an intensity ratio of 1:3:3:1. Both the width and spacing of the lines vary as the crystal orientation is changed relative to the external magnetic field. In Fig. 3 the splitting is plotted against angle for rotations about the  $a$ -axis and in Fig. 4 for rotations about the  $b$ -axis (see inset in Fig. 3 for a model of the anthracene lattice). These data are fitted by a Hamiltonian of axial symmetry for the hyperfine interaction containing an isotropic and anisotropic dipole-dipole term. This Hamiltonian is

$$H_{\text{HFS}} = a + b(3 \cos^2 \theta - 1)$$

where  $a = 14.8 \pm 1.0$  gauss,  $b = 1.8 \pm 1.0$  gauss and  $\theta$  is the angle between the external magnetic field,  $H_0$ , and an axis of symmetry lying along the  $c$ -axis of the lattice.

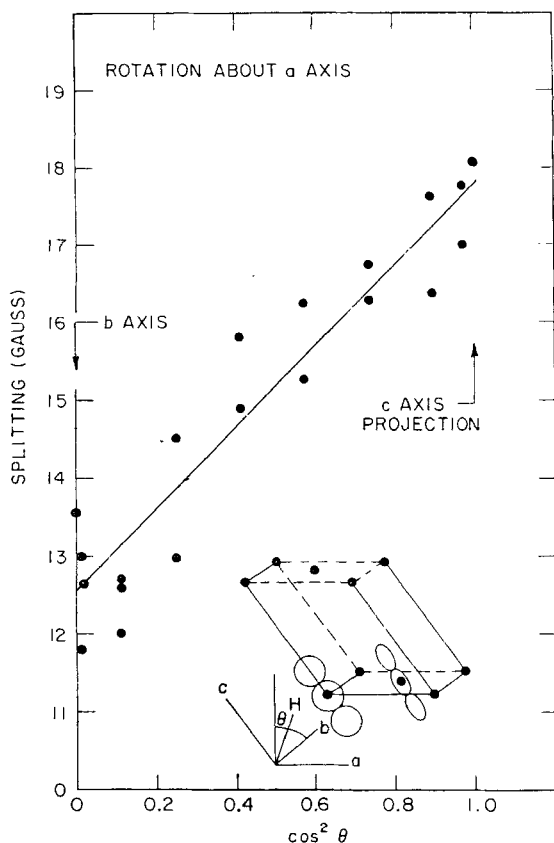


Figure 3. Hyperfine splitting *vs* angle for  $\gamma$ -irradiated anthracene. Rotation about  $a$ -axis.

Both the optical absorption and EPR spectra are stable at room temperature. When the crystal is annealed isochronally two changes take place in the optical spectrum. The first is a reduction of the radiation induced background and the second is the growth of the peaks at 6060 Å and 5350 Å; see Fig. 1. These data are

reproducible within the size of the points. As the annealing process reaches  $140^{\circ}\text{C}$  the peak at  $6320\text{ \AA}$  disappears and a peak appears at  $4950\text{ \AA}$ . At this temperature the peaks at  $6060\text{ \AA}$  and  $5350\text{ \AA}$

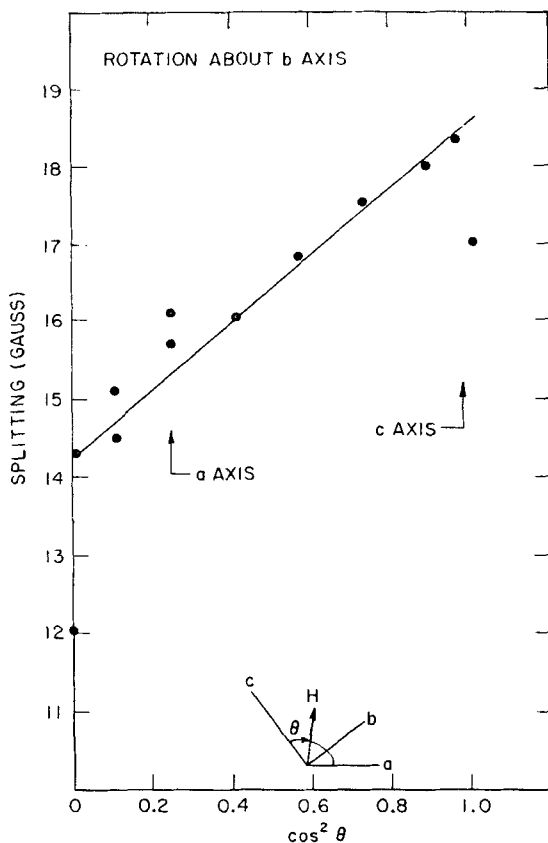


Figure 4. Hyperfine splitting *vs* angle for  $\gamma$ -irradiated anthracene. Rotation about *b*-axis.

have reached a maximum in intensity and the EPR signal has not changed (Fig. 5). The EPR data of Fig. 5 can be in error by 10–15% because the sample is removed from the cavity for annealing. Further annealing reduces the magnitude of both the optical



absorption peaks and the EPR signal. After the 170°C step of the annealing process the peak at 6060 Å has nearly vanished while the peak at 5350 Å has decreased to about one-half of its maximum height. As a result the crystal appears bright orange. Annealing to 200°C causes a decrease in both the radiation-induced background and the peaks, and the crystal becomes light yellow in

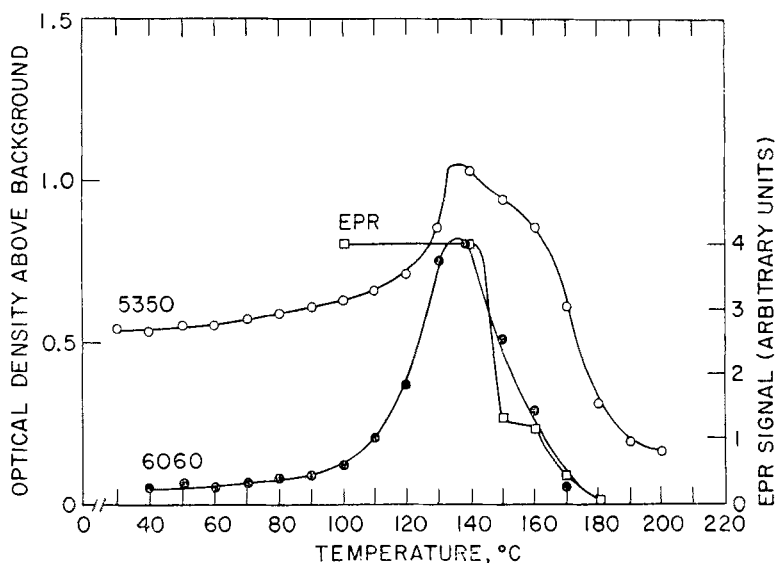


Figure 5. Optical density of 5350 Å and 6060 Å absorption peaks (left scale) and EPR signal (right scale) during 45 min isochronal annealing.

color. After the annealing step at 180°C an unresolved peak appears at 4530 Å (not shown). Also the peak at 4950 Å has shifted to shorter wavelength following the 200°C annealing, as seen in Fig. 1. The peaks at 6060 Å and 5350 Å (Fig. 5) seem to grow similarly with increasing temperature, although this is difficult to assess accurately since the 5350 Å peak was obscured to some extent by the background at the lower annealing temperatures. The 5350 Å line of Fig. 5 is therefore not necessarily an accurate description of the growth and decay of this peak. The maximum intensity of the peak at 6060 Å occurs between 130°C and 140°C

and has, at 140°C, an extinction coefficient of  $9.2 \text{ cm}^{-1}$  and a full width at half maximum of  $410 \text{ cm}^{-1}$  (0.05 eV). Nothing more can be said about the absorption intensities because of the overlap with radiation-induced background and the band edge of anthracene. The optical absorption was measured at 10°K in a crystal that had been annealed through the 140°C step but no narrowing of the peaks with temperature was observed.

In the crystals which were irradiated and annealed in vacuo, the optical and EPR spectra were identical to the spectra of the crystals irradiated in air for the same stages of annealing.

No differences between the high purity and the Harshaw crystals were observed in any of the measurements.

## Discussion

Crystals irradiated and annealed in vacuo behaved the same as all others which indicates that a surface impurity or reaction product has not diffused into the crystals to cause the absorption peaks. Gas chromatographic analysis of dissolved crystals both as-irradiated and those which had been annealed to 200°C showed no trace of any impurity. Much higher doses are probably necessary to measure radiation products by this method.

It is estimated from the signal size that for a dose of  $\sim 10^7 \text{ r}$  the number of spins contributing to the EPR signal is  $10^{17}$  per  $\text{cm}^3$ . Since no saturation of signal growth was observed to a dose of  $10^9 \text{ r}$  (approximately  $10^{19}$  spins per  $\text{cm}^3$ ) it is concluded that the effects are due to a radiation-induced defect or chemical reaction rather than a radiation activated impurity, because impurities of such a high concentration would have been detected by other techniques. Also, the similarity of the results in scintillator grade anthracene and highly purified anthracene points away from an impurity dependent effect.

Attempts were made to determine the nature of the EPR center by comparison with related molecules. Naphthalene and anthracene were irradiated with 50 keV X-rays; these have sufficient energy to ionize the molecules and create paramagnetic radicals.

No coloration or EPR signals were observed which indicates that the damage produced by  $\gamma$ -rays is more than simply the formation of radicals. Positive and negative ion radicals of many aromatic hydrocarbons have been formed by others, and their EPR spectra studied.<sup>3</sup> It is generally found that the unpaired electron spin density is spread throughout the molecule, giving rise to a spectrum consisting of many narrow lines around  $g=2$  with an overall extension in field of between 20 and 30 gauss. The total width of the EPR spectrum in the  $\gamma$ -irradiated anthracene described here (Fig. 2) is roughly three to four times as great as the overall width observed in both positive and negative anthracene radicals in solution.<sup>3</sup> It is not expected that the disparity in the hyperfine structure between anthracene radicals in solution and in solid would be a result of the medium itself because both theory and experiments indicate that the wave functions are tightly bound to the molecule, and therefore interactions would be small.<sup>4</sup> No radicals of possible degradation products of anthracene which have been studied,<sup>3</sup> e.g., naphthalene, have exhibited a spectrum approximate to that observed in  $\gamma$ -irradiated anthracene. It seems unlikely that a radical of anthracene or any simple degradation product is the source of the EPR signal.

The spectrum found in  $\gamma$ -irradiated anthracene is that expected from three equivalent spin 1/2 nuclei coupling with an unpaired electron. An attractive concept for this pattern is a methyl radical since other measurements show the intensity ratios and hyperfine splittings for the methyl radical to be approximately the same as  $\gamma$ -irradiated anthracene.<sup>5</sup> As a test of the hypothesis that methyl radicals are formed and become attached to anthracene molecules during  $\gamma$ -irradiation, 2-methyl anthracene and 9-methyl anthracene were given sufficient X-radiation to produce paramagnetic centers, but no EPR spectra were detected. Pure anthracene was also subjected to X-radiation but no EPR signal was found. Powders of anthracene, 2-methyl anthracene and 9-methyl anthracene were  $\gamma$ -irradiated and their EPR spectra are shown in Fig. 6. The similarity in the observed spectra tends to rule out the possibility of the defects being directly connected to the anthracene rings since

the addition of a methyl group would be expected to perturb the EPR spectrum strongly. It is gratifying that the methyl radical must be rejected since investigations have shown that it cannot be retained in other crystals above liquid nitrogen temperatures.<sup>5</sup>

Other similar aromatic hydrocarbons were  $\gamma$ -irradiated and their EPR spectra observed. Figure 7 shows the spectra for powders of

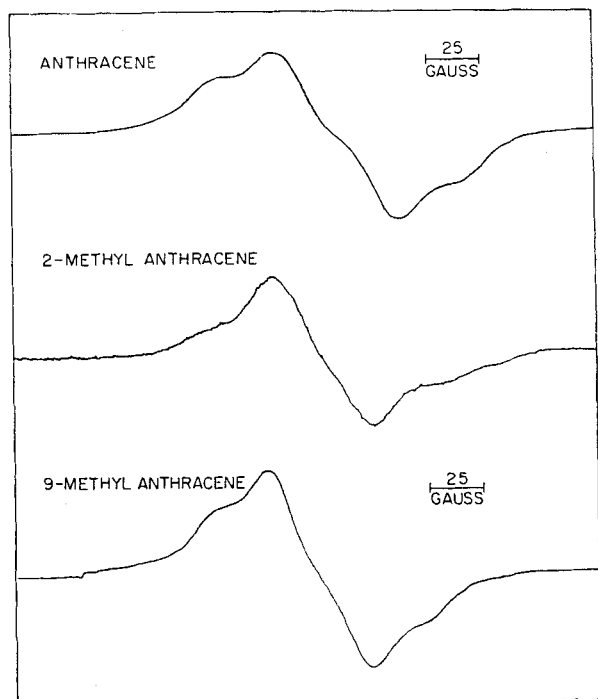


Figure 6. EPR absorption derivatives for powders of  $\gamma$ -irradiation materials.

chrysene, tetracene, naphthalene and single crystal phenanthrene. Our phenanthrene results are in disagreement with previously reported spectra.<sup>6</sup>

It is well known that heavy  $\gamma$ -irradiation eventually causes polymerization of hydrocarbons.<sup>7</sup> In view of this and the results described above it seems appropriate to suggest that the observed

center, rather than being a radical of an anthracene molecule, or a fragment of it, is formed by a cross-linking of two anthracene molecules. Figure 8 shows a possible model for such cross-linking. This model fits the geometry of the anthracene lattice exactly and

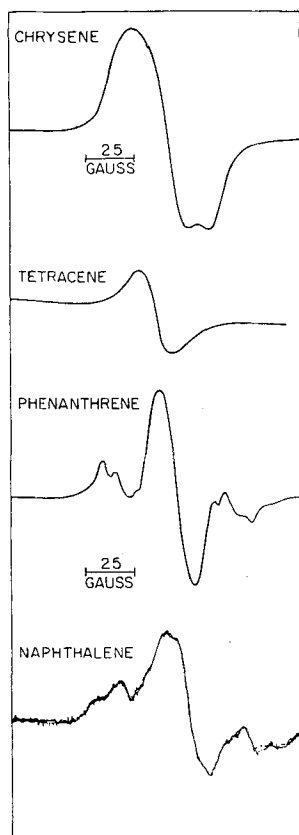


Figure 7. EPR absorption derivatives for powders of  $\gamma$ -irradiation materials.

is consistent with the resonance spectra. The four-line spectrum would arise from the hyperfine interaction of the unpaired electron with protons on the carbon atoms which form the linear cross-link chain, while the width of each line is attributed to interaction with the two remaining rings on each side.

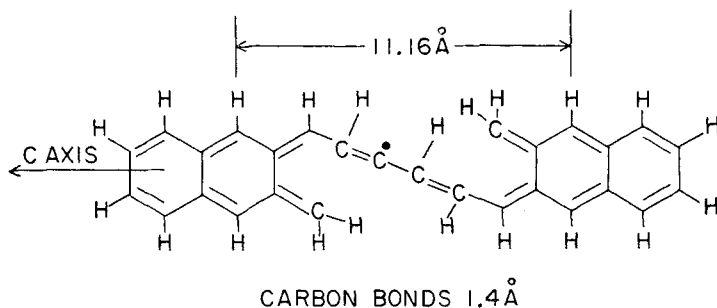


Figure 8. Proposed cross-linking of anthracene molecules. Black dot is unpaired electron.

### Acknowledgments

We thank F. Vasquez for help in running the angular dependence of the EPR spectrum of anthracene. Also, we acknowledge helpful discussions with Dr. G. J. Dienes, Dr. P. J. Herley and Dr. S. Z. Weisz.

### REFERENCES

1. See for example, Sloan, G. J., *Molecular Crystals* **1**, 161 (1966).
2. Hoesterey, D. C. and Letson, G. M., *J. Phys. Chem. Solids* **24**, 1609 (1963).
3. de Boer, E., *J. Chem. Phys.* **25**, 190 (1956); de Boer, E. and Weissman, S. I., *J. Am. Chem. Soc.* **80**, 4549 (1958); Weissman, S. I., de Boer, E., and Conradi, J. J., *J. Chem. Phys.* **26**, 963 (1956); Carrington, A., Drawnieks, F., and Symons, M. C. R., *J. Chem. Soc.* 947 (1959); Fessenden, R. W. and Schuler, R. H., *J. Chem. Phys.* **39**, 2147 (1963).
4. LeBlanc, O. H., *J. Chem. Phys.* **35**, 1275 (1961).
5. Jen, C. K., Foner, S. N., Cochran, E. L., and Bowers, V. A., *Phys. Rev.* **112**, 1169 (1958); Piette, L. H., in *NMR and EPR Spectroscopy*, Pergamon Press, London 1960; Miyagawa, I. and Itoh, K., *J. Chem. Phys.* **36**, 2157 (1962).
6. Bouldin, W. V., *Bull. Am. Phys. Soc.* **11**, 514 (1966) and private communication; Hankla, R. H., Thesis, Vanderbilt University 1966 (unpublished).
7. See for example, Hall, K. L., Bolt, R. O., and Carroll, J. G., in *Radiation Effects on Organic Materials*, Academic Press, New York (1963), p. 85.